Dynamically stable two- and four-droplet solitons in a very strongly dipolar NaCs condensate

S. K. Adhikari *

Instituto de Física Teórica, UNESP - Universidade Estadual Paulista, 01.140-070 São Paulo, São Paulo, Brazil

(Received 3 February 2025; accepted 1 May 2025; published 19 May 2025)

A strongly dipolar Bose-Einstein condensate (BEC) of Dy atoms could sustain different types of states not possible in a nondipolar BECs. Motivated by the observation of a very strongly dipolar condensate of NaCs molecules [N. Bigagli *et al.*, Nature (London) **631**, 289 (2024)], with dipolar interaction stronger by more than an order of magnitude compared with that of Dy atoms, we demonstrate that, in a very strongly dipolar NaCs BEC, it is possible to have a two- and a four-droplet metastable soliton, axially free along the polarization z direction. In this study, we employ imaginary-time propagation of an improved mean-field model, including the Lee-Huang-Yang interaction. The dipolar solitons are subject to an expulsive Gaussian potential at the center and a harmonic potential, both acting in the x-y plane. The phase-coherent solitons, possessing the isolated droplets, are free to move along the z-axis without any relative motion between the droplets. The dynamical stability and mobility of these solitons are demonstrated by real-time propagation employing the converged imaginary-time wave function as the initial state.

DOI: 10.1103/PhysRevE.111.054212

I. INTRODUCTION

The observation of dipolar Bose-Einstein condensates (BECs) of ^{52}Cr [1–6], ^{166}Er [7], ^{168}Er [8], and ^{164}Dy [9–12] atoms with large magnetic dipole moments opened a new avenue of research. More recently, a very strongly dipolar BEC of NaCs molecules was observed [13]. The dipolar length of Dy atoms, which is a measure of the strength of the dipolar interaction, viz. Eq. (3), has the value $a_{\rm dd} = 130.8a_0$, where a_0 is the Bohr radius. However, the effective electrical dipole moment of a NaCs molecule can be controlled by the microwave-shielding technique [14], which allows for an NaCs molecule of very large dipolar length in the range $a_{\rm dd} = 1000a_0$ to $25\,000a_0$ [13], much larger than the dipolar length of Dy atoms.

The most remarkable phenomenon in a strongly dipolar harmonically trapped BEC is the observation of a single droplet [15,16] of a size much smaller than the harmonic oscillator trap length, in addition to a self-bound droplet in free space [15,17,18]. With the increase in the number of atoms in the harmonically trapped dipolar BEC, multiple droplets are formed [15,19–22].

Another important research area in BECs is the statics and dynamics of quantum solitons. A soliton or solitary wave is a one-dimensional (1D) self-reinforcing wave packet that maintains its shape due to a cancellation of nonlinear attraction and dispersive repulsion, while it propagates at a constant velocity [23,24]. The 1D soliton is analytic and obeys strict conservation laws (energy, momentum), and maintains its shape after a collision. Solitons have been studied in water waves, BECs [23], and a general nonlinear medium [25] including nonlinear optics [24]. In three dimensions, the realization of such a propagating soliton is possible by confining a BEC in the x-y plane by a trap and allowing it to propagate freely along the untrapped z direction [26], thus creating a (quasi-1D configuration. A quasi-1D soliton was predicted [26] for attractive interaction and created in a BEC of ^{7}Li [27,28] and ^{85}Rb [29] atoms. There have also been many studies of quasi-1D solitons in dipolar BECs under different conditions [30–33]. Quasi-1D solitons were also found [34–36] in a spin-orbit (SO)-coupled BEC equilibrated by an external trap and SO-coupling interaction. In addition, quasi-1D solitons are also possible [37] in a dipolar BEC. There are numerous examples of similar quasi-1D solitons in BECs [38–45]. Nevertheless, all quasi-1D solitons are formed in the presence of a trap in the x-y plane and hence are numeric and only obey the conservation laws approximately.

In this paper, we address the interesting question, "In view of the multiple droplet formation in a trapped dipolar BEC [19–22,46], is it possible to have a multiple-droplet quasi-1D soliton in a strongly dipolar BEC?" To this end, we demonstrate that it is indeed possible to have metastable quasi-1D two- or four-droplet solitons in a very strongly dipolar BEC of NaCs molecules free to move along the polarization z direction. The quasi-1D trap consists of a harmonic one in the x-y plane and an expulsive Gaussian potential at the center of the same plane, with no trap in the z direction. The two- and four-droplet solitons are phase coherent and can move as a unified whole along the z-axis without any relative motion between the spatially separated droplets. These quasi-1D solitons, like all quasi-1D BEC solitons, stabilized by the combined effect of the confining trap and the long-range dipolar interaction, are numeric in nature and are not analytic solitons in the strict mathematical sense; the term soliton is being used more loosely here to highlight their stability and mobility. The energy of the two-droplet soliton is smaller than that of the four-droplet soliton, and the lowest-energy stable soliton is a one-droplet soliton. As the dipolar interaction is reduced, by decreasing the number of molecules or the

*Contact author: sk.adhikari@unesp.br

effective electric dipole moment of a molecule, the droplets of the metastable soliton join together to form a stable soliton of a single droplet.

In theoretical investigations, employing the mean-field Gross-Pitaevskii (GP) model, a trapped dipolar BEC collapses in 3D for a strong dipolar interaction beyond a critical value [6,47–50]. However, when an improved Lee-Huang-Yang [51] (LHY) interaction, appropriate for a dipolar system [52–54], is included in this model, the collapse can be stopped [17,55]. As the number of atoms (or molecules) gradually increases in a trapped dipolar BEC in this model, a stable droplet, and eventually, multiple droplets, are formed [15,16,56]. Using this improved mean-field model, we show that, with an appropriate confining trap in the x-y plane alone, a very strongly dipolar BEC of NaCs molecules can sustain two- and four-droplet solitons. The self-bound quantum droplets in free space [17,18] are mobile in all directions, droplets in a harmonically trapped dipolar BEC [15,16] are immobile, whereas the present droplet solitons are mobile only along the polarization z direction.

In Sec. II, we present the improved mean-field model for the very strongly dipolar BEC of NaCs molecules with repulsive contact and long-range dipolar interactions, including an appropriate LHY interaction. In Sec. III, we display numerical results for the formation of the metastable two- and four-droplet solitons. The stationary states of the metastable solitons are obtained by imaginary-time propagation, and their propagation dynamics are studied by real-time propagation. In Sec. IV, we present a brief summary of the investigation.

II. IMPROVED MEAN-FIELD MODEL

We consider a BEC of N dipolar molecules, polarized along the z-axis, interacting through the following molecular dipolar and contact interactions [1,57,58]:

$$V(\mathbf{R}) = \frac{{\rm d_{eff}}^2}{4\pi\epsilon_0} U_{\rm dd}(\mathbf{R}) + \frac{4\pi\hbar^2 a}{m}\delta(\mathbf{r}-\mathbf{r}'), \tag{1}$$

$$U_{\rm dd}(\mathbf{R}) = \frac{1-3\cos^2\theta}{|\mathbf{R}|^3}, \tag{2}$$

where m is the mass of a molecule, a is the intermolecular s wave scattering length, $\rm d_{eff}$ is the effective electric dipole moment of each NaCs molecule, and ϵ_0 is the permittivity of vacuum. Here, $\mathbf{r} \equiv \{\mathbf{x}, \mathbf{y}, \mathbf{z}\}$ and $\mathbf{r}' \equiv \{\mathbf{x}', \mathbf{y}', \mathbf{z}'\}$ are the position vectors of the dipolar molecules and θ is the angle made by the relative position vector $\mathbf{R} \equiv \mathbf{r} - \mathbf{r}'$ with the polarization z direction. The following dipolar length $a_{\rm dd}$ determines the strength of the dipolar interaction

$$a_{\rm dd} = \frac{m{\rm d_{eff}}^2}{12\pi\hbar^2\epsilon_0}, \tag{3}$$

whereas the scattering length a determines the strength of the contact interaction.

In this paper, we employ an improved mean-field model incorporating the LHY interaction [51] appropriately modified for dipolar atoms and molecules [52,53]. The formation of a two- or four-droplet soliton mobile along the polarization z direction is described by the following 3D GP equation, including the LHY interaction [1,56–59]:

$$\begin{aligned} i\hbar\frac{\partial\psi(\mathbf{r},t)}{\partial t} = \Bigg[&-\frac{\hbar^2}{2m}\nabla^2 + U(\mathbf{r}) + \frac{4\pi\hbar^2}{m}aN|\psi(\mathbf{r},t)|^2 \\ &+ \frac{3\hbar^2}{m}a_{\rm dd}N\int U_{\rm dd}(\mathbf{R})|\psi(\mathbf{r}',t)|^2 d\mathbf{r}' \\ &+ \frac{\gamma_{\rm LHY}\hbar^2}{m}N^{3/2}|\psi(\mathbf{r},t)|^3\Bigg]\psi(\mathbf{r},t), \end{aligned} \tag{4}$$

$$U(\mathbf{r}) = \frac{m\omega^2}{2}(x^2+y^2) + V_0\exp\left[-\frac{x^2+y^2}{\delta^2}\right], \tag{5}$$

where the trapping potential $U(\mathbf{r})$ is a combination of a weak confining harmonic and an expulsive Gaussian potential, both in the x-y plane and the dipolar system is free to move along the polarization z direction; ω is the angular frequency of the harmonic trap; and V_0 and δ are the strength and width of the Gaussian potential, respectively. The repulsive Gaussian potential keeps the droplets of the soliton apart and allows the formation of a metastable two- or four-droplet dipolar soliton in the x-y plane with long extension in the z direction. The wave function is normalized as $\int|\psi(\mathbf{r},t)|^2 d\mathbf{r} = 1$. The coefficient of the LHY interaction $\gamma_{\rm LHY}$ in Eq. (4) is given by [52,53,56]

$$\gamma_{\rm LHY} = \frac{128}{3}\sqrt{\pi a^5}Q_5(\varepsilon_{\rm dd}), \quad \varepsilon_{\rm dd} = \frac{a_{\rm dd}}{a}, \tag{6}$$

where the auxiliary function $Q_5(\varepsilon_{\rm dd})$ is given by $Q_5(\varepsilon_{\rm dd}) = \int_0^1 dx(1-\varepsilon_{\rm dd}+3x^2\varepsilon_{\rm dd})^{5/2}$. This function is evaluated as [56]

$$\begin{aligned} Q_5(\varepsilon_{\rm dd}) = \frac{(3\varepsilon_{\rm dd})^{5/2}}{48}\mathcal{R}\Bigg[&(8+26\eta+33\eta^2)\sqrt{1+\eta} \\ &+ 15\eta^3\ln\left(\frac{1+\sqrt{1+\eta}}{\sqrt{\eta}}\right)\Bigg], \quad \eta = \frac{1-\varepsilon_{\rm dd}}{3\varepsilon_{\rm dd}}, \end{aligned} \tag{7}$$

where $\mathcal{R}$ denotes the real part. Equation (7) for $Q_5(\varepsilon_{\rm dd})$ has been used in the numerical calculation in this paper.

We can rewrite Eq. (4) in the following dimensionless form by scaling lengths in units of $l_0 = \sqrt{\hbar/m\omega_0}$, time in units of $t_0 = \omega_0^{-1}$, angular frequency ω in units of ω_0, energy and V in units of $\hbar\omega_0$, and density $|\psi|^2$ in units of l_0^{-3}, where ω_0 is a reference angular frequency:

$$\begin{aligned} i\frac{\partial\psi(\mathbf{r},t)}{\partial t} = \Bigg[&-\frac{1}{2}\nabla^2 + U(\mathbf{r}) + 4\pi aN|\psi(\mathbf{r},t)|^2 \\ &+ 3a_{\rm dd}N\int U_{\rm dd}(\mathbf{R})|\psi(\mathbf{r}',t)|^2 d\mathbf{r}' \\ &+ \gamma_{\rm LHY}N^{3/2}|\psi(\mathbf{r},t)|^3\Bigg]\psi(\mathbf{r},t), \end{aligned} \tag{8}$$

$$U(\mathbf{r}) = \frac{1}{2}\omega^2(x^2+y^2) + V_0\exp\left[-\frac{x^2+y^2}{\delta^2}\right], \tag{9}$$

where, and in the following, without any risk of confusion, we use the same symbols to denote the new scaled variables. The normalization in the scaled variables remains unchanged: $\int|\psi(\mathbf{r},t)|^2 = 1$.

We can also derive Eq. (8) from the variational rule $i\partial\psi/\partial t = \delta E/\delta\psi^*$, where E is an energy functional (energy

per molecule of a stationary state) given by

$$E = \int d\mathbf{r}\Big[\frac{1}{2}|\nabla\psi(\mathbf{r})|^2 + U(\mathbf{r})|\psi(\mathbf{r})|^2 + \frac{3}{2}a_{\rm dd}N|\psi(\mathbf{r})|^2\int U_{\rm dd}(\mathbf{R})|\psi(\mathbf{r}')|^2 d\mathbf{r}' + 2\pi N a|\psi(\mathbf{r})|^4 + \frac{2\gamma_{\rm LHY}}{5}N^{3/2}|\psi(\mathbf{r})|^5\Big]. \quad (10)$$

III. NUMERICAL RESULTS

To obtain the very strongly dipolar two- and four-droplet solitons of NaCs molecules, we solve the partial differential GP equation [Eq. (8)], numerically, using FORTRAN/C programs [57,60] or their open-multiprocessing versions [61,62], employing the split-time-step Crank-Nicolson method using the imaginary-time propagation rule [63]. It is difficult to treat numerically the divergent $1/|\mathbf{R}|^3$ term in the dipolar potential [Eq. (2)] in configuration space. To circumvent this problem, this term in the nonlocal dipolar interaction integral in Eq. (8) is evaluated in the momentum $\mathbf{k}$ space by a Fourier transformation [57]. After the problem is solved in the momentum space, the desired solution in configuration space is obtained by a backward Fourier transformation.

For the appearance of a quasi-1D two- or four-droplet soliton, we need a very strongly dipolar BEC of NaCs molecules with $a_{\rm dd} \gg a$ [16]. In this study, we take $a_{\rm dd} = 2000a_0$ and $a = 100a_0$, which makes the system very strongly dipolar. Although we use NaCs molecules in this study, we do not include the effect of microwave shielding, which is beyond the scope of this investigation. For NaCs molecules m(NaCs) $\approx 156 \times 1.66054 \times 10^{-27}$ kg, we take the reference frequency $\omega_0 = 2\pi \times 180$ Hz; consequently, the unit of length $l_0 = \sqrt{\hbar/m\omega_0} = 0.600$ μm and unit of time $t_0 = \omega_0^{-1} = 0.88$ ms. The trap parameters in Eq. (5) are taken as $\omega = 2\pi \times 54$ Hz, $V_0/h = 1800$ Hz, and $\delta = \sqrt{2}l_0 \approx 0.8485$ μm. Here, l_0 and ω_0 are scaling parameters used in writing the dimensionless equations and have no effect on the final result.

Although metastable, these solitons can be obtained by imaginary-time propagation, as they possess distinct spatial symmetry properties; an imaginary-time propagation scheme usually preserves the spatial symmetry of the initial state. The metastable two- and four-droplet solitons are dynamically stable, and this dynamics can be studied by real-time propagation. Given a push, these solitons are able to travel along the polarization z direction without any visible deformation with a uniform velocity, as is demonstrated.

To obtain a four-droplet soliton easily by the imaginary-time propagation routine, we took the initial state as four droplets placed at the corners of a square whose center is at the origin, for example, at $\{x, y\} = \{\pm\alpha, \pm\alpha\}$. To obtain a two-droplet state the two droplets in the initial state are placed at $\{x, y\} = \{\pm\alpha, 0\}$. Because of the distinct spatial symmetry of four- and two-droplet solitons, these states are remarkably stable and a higher-energy four-droplet soliton cannot easily decay to a lower-energy two-droplet soliton, provided we employ an accurate numerical scheme with small time and space steps with a large number of space discretization points. In an approximate numerical scheme, this may not be true,

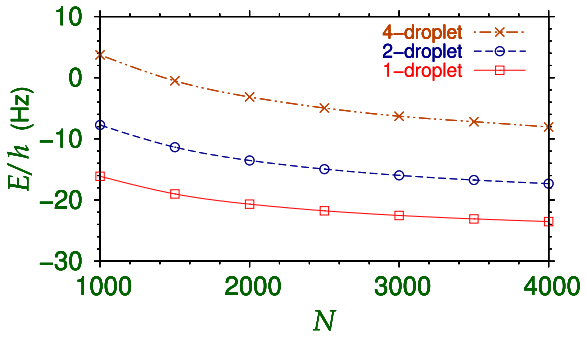

FIG. 1. Energy per atom E/h in Hz of four-droplet, two-droplet and one-droplet solitons for different numbers of NaCs molecules N. The points are the numerical results, which are joined by the lines to guide the eye. The dipolar length and scattering length are $a_{\rm dd} = 2000a_0$, $a = 100a_0$, respectively. The trap parameters, viz. Eq. (5), are $\omega = 2\pi \times 54$ Hz, $V_0/h = 1800$ Hz, $\delta = \sqrt{2}l_0$, $l_0 = 0.6$ μm. These parameters are the same in all figures.

and a four-droplet initial state may lead to a two-droplet, or even a one-droplet, soliton. We take the space discretization steps along x, y, z directions as $dx = dy = 0.1, dz = 0.125$, respectively, which is adequate for our study. The employed time steps were $dt = 0.1(dx \times dy \times dz)^{2/3}$ in imaginary-time propagation and $dt = 0.025(dx \times dy \times dz)^{2/3}$ in real-time propagation. The number of space discretization points in x and y directions were $N_x = N_y = 257$, and that in the z direction could be as large as $N_z = 769$.

We find that the solitons can be found for a relatively small number of molecules. In Fig. 1, we display the energy per molecule [Eq. (10)] E/h for the four-, two-, and one-droplet solitons for different numbers of molecules N from 1000 to 4000. For a fixed number of molecules, the energy E/h of the four-droplet (two-droplet) soliton is larger than that of the two-droplet (one-droplet) soliton. The energy E/h, and the total energy of the soliton NE/h, for a fixed number of droplets, decreases as the number of molecules increases. For the present set of parameters, in imaginary-time propagation, we could not stabilize a three-droplet soliton or a soliton with more than four droplets. In imaginary-time propagation, these states eventually decay to a two-droplet or one-droplet soliton. For a different set of interaction and trap parameters, it might be possible to stabilize the solitons with a different number of droplets, which could be a study of future interest. The repulsive dipolar interaction in the x-y plane and the expulsive Gaussian potential at the center keep the droplets apart while the harmonic trap binds them in a metastable state to form a two-droplet or four-droplet soliton. However, if we take a more complex trap in the x-y plane, consisting of multiple barriers, preliminary study indicates that the number of droplets in the soliton will increase, which is beyond the scope of this investigation. The interaction between solitons and droplets depends on the relative phase. In the present case of phase-coherent solitons, the phase between the different droplets is zero.

The confining potential [Eq.(9)] in the x-y plane is one with ring topology. In place of using the appropriately placed four or two droplets in the initial state in imaginary-time propagation, if we use a Gaussian function as the initial state,

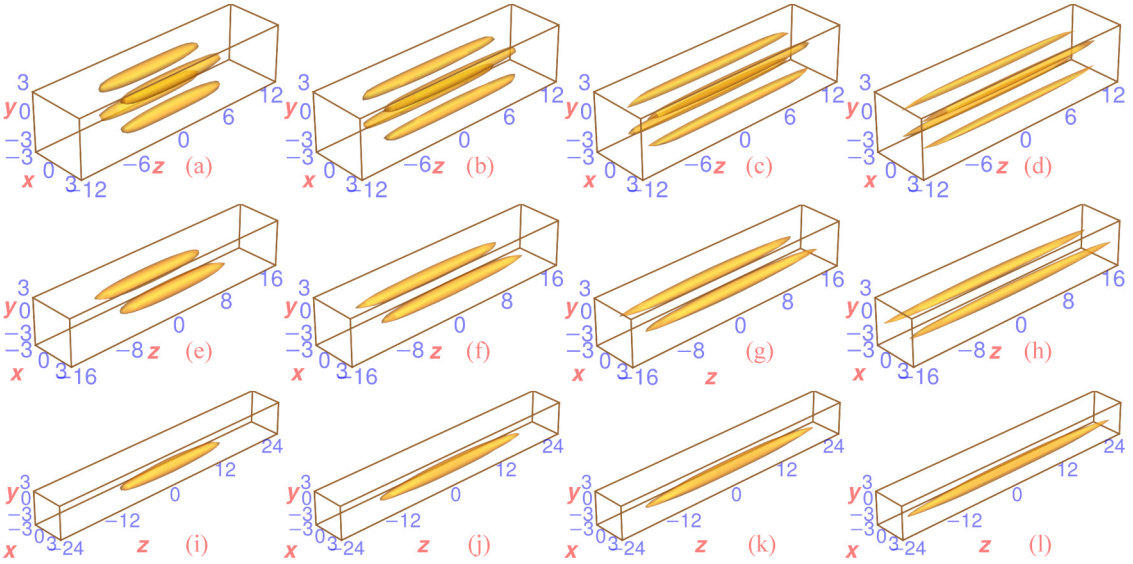

FIG. 2. Isodensity plot of normalized density $|\psi(x, y, z)|^2$ ($\int |\psi(\mathbf{r})|^2 d\mathbf{r} = 1$) of a four-droplet soliton of $N =$ (a) 1000, (b) 2000, (c) 3000, and (d) 4000 NaCs molecules; of a two-droplet soliton of $N =$ (e) 1000, (f) 2000, (g) 3000, and (h) 4000 molecules; and of an one-droplet soliton of $N =$ (i) 1000, (j) 2000, (k) 3000, and (l) 4000 molecules. The unit of lengths is μm. The density on contour is $\rho_{\rm cont} = 4.6 \times 10^9$ cm^{-3}. As the net density of molecules is $N|\psi(x, y, z)|^2$, the density of NaCs molecules on contour in these cases are $N\rho_{\rm cont}$.

we obtain a highly metastable hollow cylindrical soliton state with ring topology. This state has higher energy than the four-, two-, and one-droplet solitons, viz. Fig. 1. With a prolonged time propagation, the hollow cylindrical soliton evolves into the four-droplet soliton (result not shown). However, it might be possible to stabilize a metastable hollow cylindrical soliton with ring topology for a different set of parameters, which could be a very interesting work of future investigation.

The evolution of the few-droplet soliton for different numbers of droplets and different numbers of molecules is best illustrated through an isodensity plot of the solitons. In Fig. 2, we show the evolution of a four-droplet soliton by the isodensity plot of normalized density $|\psi(x, y, z)|^2$ for (a) $N = 1000$, (b) $N = 2000$, (c) $N = 3000$, and (d) $N = 4000$ NaCs molecules. As the number of molecules increases from Fig. 2(a) through (d), the system becomes increasingly dipolar and the length of the droplets along the polarization z direction increases, although the spatial extension in the x-y plane of the four-droplet soliton remains essentially the same for different N. The spatial extension in the x-y plane is essentially controlled by the minimum of the confining trap [Eq. (9)] in that plane. If we had plotted the net density $N|\psi(x, y, z)|^2$, in place of normalized density $|\psi(x, y, z)|^2$, and used the same cutoff density in the plots, both the length of a droplet and its section in the x-y plane will increase, as N increases, as we see in the following through a plot of the net integrated two-dimensional (2D) [64] and 1D densities. The same trend continues in the case of a two-droplet soliton as shown in Fig. 2 for (e) $N = 1000$, (f) $N = 2000$, (g) $N = 3000$, and (h) $N = 4000$ molecules and a one-droplet soliton as shown in Fig. 2 for (i) $N = 1000$, (j) $N = 2000$, (k) $N = 3000$, and (l) $N = 4000$ molecules. For the same number N of molecules, each droplet of a two-droplet soliton in Fig. 2 is longer along the z direction than that of a four-droplet soliton. This is because, for a fixed N, each droplet of a two-droplet soliton has twice as many molecules compared with that of a four-droplet soliton. A larger number of molecules in each droplet of a two-droplet soliton leads to a larger dipolar interaction responsible for generating a longer droplet. From the isodensity plot of a one-droplet soliton of Fig. 2, we find that these droplets are longer than both a four-droplet and a two-droplet soliton because of the largest number of molecules in a one-droplet soliton. The dipolar interaction in a one-droplet soliton is the largest, which makes the one-droplet soliton the longest along the polarization z direction.

The different spatial extensions of these solitons can be studied employing the integrated 2D density in the x-y plane $n_{\rm 2D}(x, y)$ and the integrated 1D density in the z direction $n_{\rm 1D}(z)$ defined, respectively, by

$$n_{\rm 2D}(x, y) = \int_{-\infty}^{\infty} dz |\psi(x, y, z)|^2, \tag{11}$$

$$n_{\rm 1D}(z) = \int_{-\infty}^{\infty} dx \int_{-\infty}^{\infty} dy |\psi(x, y, z)|^2. \tag{12}$$

The integrated 2D density $n_{\rm 2D}(x, y)$ is useful to study the spatial extension (or localization) of the soliton in the x-y plane, the integrated 1D density $n_{\rm 1D}(z)$ is useful to study the linear extension of the same along the z direction.

In Fig. 3, we illustrate the net integrated 2D density $Nn_{\rm 2D}(x, y)$ through a contour plot of the same in the x-y plane of the four-droplet solitons of Fig. 2 of $N =$ (a) 1000, (b) 2000, (c) 3000, and (d) 4000 NaCs molecules. The same for the two-droplet solitons in Fig. 2 are shown in Fig. 3 for $N =$ (e) 1000, (f) 2000, (g) 3000, and (h) 4000 NaCs molecules. As the number of molecules N increases in plots in Figs. 3(a)–3(d) of a four-droplet soliton, the droplets not only become fatter, with larger cross-section in the x-y plane, but also have larger molecule density. The same is true about a two-droplet soliton, shown in Figs. 3(e)–3(h). However, the maximum molecule density and the cross section of a single droplet in

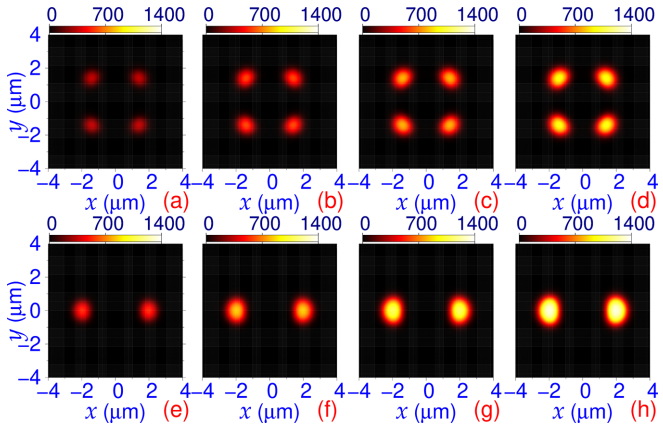

FIG. 3. Contour plot of net integrated 2D density $n(x, y) \equiv Nn_{2D}(x, y)$ $[\int_{-\infty}^{\infty} dx \int_{-\infty}^{\infty} dy n(x, y) = N]$ versus $\{x, y\}$ for four-droplet solitons in Fig. 2 for $N =$ (a) 1000, (b) 2000, (c) 3000, and (d) 4000 NaCs molecules. The same for two-droplet solitons in Fig. 2 for $N =$ (e) 1000, (f) 2000, (g) 3000, (h) 4000 NaCs molecules. The unit of densities in the color box is μm^{-2}.

a two-droplet soliton in Figs. 3(e)–3(h) are larger than those in Figs. 3(a)–3(d) in a four-droplet soliton, respectively, for $N =$ 1000, 2000, 3000, and 4000, which is reasonable as each droplet in a two-droplet soliton contains twice as many molecules as in a four-droplet soliton for a fixed N.

In Fig. 4, we display the net integrated 1D density $Nn_{1D}(z)$ through a plot of the same versus z for (a) a four-droplet soliton and (b) a two-droplet soliton for $N =$ 1000, 2000, 3000, and 4000, which also reveals some relevant information. In a four-droplet or two-droplet soliton, the length along the z direction increases with the number of molecules N. Also, for a fixed N, a two-droplet soliton is longer along the z direction than a four-droplet soliton, as each droplet in the former has twice as many molecules compared with the same in the latter.

In a four-droplet or a two-droplet soliton, the length along z direction l_z and cross section in the x-y plane σ_{xy} of a single droplet, as well as the maximum density of molecules $d_{\max}$ in a single droplet, increase as the number of molecules N increases. Also, for a fixed N, the dimensions l_z and σ_{xy} and the density $d_{\max}$ are larger for a two-droplet soliton than those of a four-droplet soliton.

From Fig. 1, we find that the two-droplet and four-droplet solitons are excited states, whereas the ground state is a one-droplet soliton. But these states have distinct spatial symmetry properties, which attributes remarkable stability properties to these states. To illustrate this stability further, we investigate the uniform motion of these solitons along z direction, which is the fundamental property of a soliton. To set these solitons in uniform motion along the z direction with a velocity v, the converged wave function obtained by imaginary-time propagation is multiplied by a prefactor $\exp(ivz)$, and the resultant wave function is then used as the initial wave function in real-time propagation. In the ideal case of infinitely small space and time steps, the real-time dynamics generates a moving soliton of velocity v. But in actual calculation with a finite space and time step, the generated uniform velocity is slightly smaller than v.

To test the dynamical stability and mobility of the four- and two-droplet solitons, we consider the converged imaginary-time wave functions corresponding to the four-droplet soliton of $N = 3000$ molecules, viz. Fig. 2(c), and the two-droplet soliton of $N = 1000$ molecules, viz. 2(e), respectively, multiply these by the phase factor $\exp(ivz)$, and use as the initial function in real-time propagation during an interval of time 5 ms. In Fig. 5(a), we illustrate the contour plot of the net integrated 2D density $n(x, y) \equiv Nn_{2D}(x, y)$ versus x, y of the four-droplet soliton of $N = 3000$ NaCs molecules as obtained by real-time propagation at $t = 5$ ms. In Fig. 5(b), we display the net integrated 1D density $n(z) \equiv Nn_{1D}(z)$ along z direction at $t = 5$ ms as obtained by real-time propagation (Re) and compare with the initial integrated 1D density $n(z)$ as obtained by imaginary-time propagation (Im). We needed to translate the real-time profile by a distance $z = z_0 = 23.5$ μm along the z direction so that the peak of the densities of real- and imaginary-time results coincide in Fig. 5(b). Hence, the four-droplet soliton has moved a distance of $z_0 = 23.5$ μm in 5 ms, resulting in a velocity of $v_0 = 4.7$ mm/s. In Fig. 5(c), we show this propagation of the four-droplet soliton through a plot of the net integrated 1D density $Nn(z, t)$ versus z and t during the uniform linear motion along the z-axis with the velocity of 4.7 mm/s. Similarly, in Fig. 5(d), we present the contour plot of the net integrated 2D density $n(x, y)$ of the two-droplet soliton of $N = 1000$ NaCs molecules after uniform linear motion during 5 ms. The net integrated 1D density $n(z)$ of the same at $t = 5$ ms (Re) is compared with the initial density (Im) in Fig. 5(e). In Fig. 5(f), we present the time evolution of the net integrated 1D density $n(z, t)$ during this linear motion. We attributed the same velocity (4.7 mm/s) and same displacement (23.5 μm) of the four- and the two-droplet solitons in Figs. 5(a)–5(c) and 5(d)–5(f), respectively.

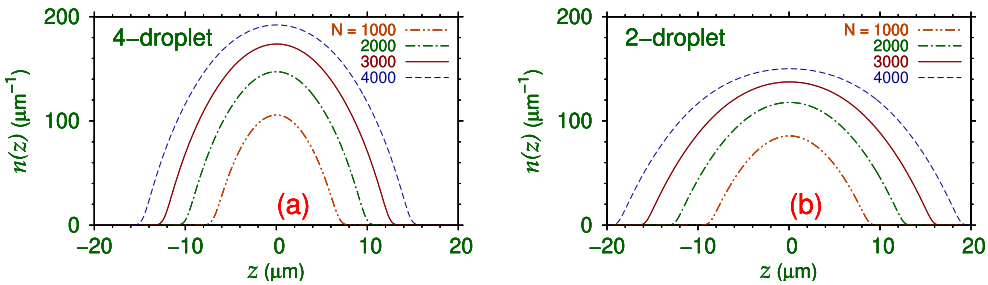

FIG. 4. Net integrated 1D density $n(z) \equiv Nn_{1D}(z)$ $[\int_{-\infty}^{\infty} dz n(z) = N]$ for (a) a four-droplet and (b) a two-droplet soliton in Fig. 2, for $N =$ 1000, 2000, 3000, and 4000 NaCs molecules.

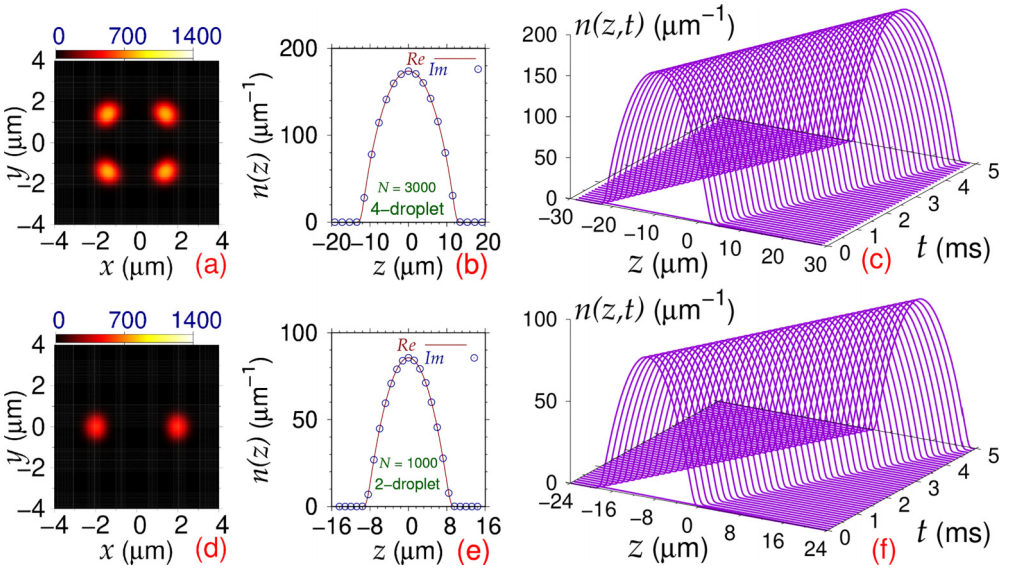

FIG. 5. Contour plot of (a) net integrated 2D density $n(x, y) \equiv Nn_{2D}(x, y)$ and plot of (b) net integrated 1D density $n(z) \equiv Nn_{1D}(z)$ (*Re*) the four-droplet soliton of $N = 3000$ NaCs molecules, viz. Fig. 2(c), after uniform motion along the z-axis during 5 ms. (b) The initial imaginary-time profile (*Im*). Both profiles are centralized at $z = 0$ in (b). (c) Time evolution of net integrated 1D density $n(z, t)$ during the uniform motion of the four-droplet soliton. Contour plot of (d) net integrated 2D density $n(x, y)$ and plot of (e) net integrated 1D density $n(z)$ of the two-droplet soliton of $N = 1000$ NaCs molecules, viz. Fig. 2(e), after uniform motion along the z-axis during 5 ms. (f) Time evolution of net integrated 1D density $n(z, t)$ during the uniform motion of the two-droplet soliton.

The integrated 1D and 2D profiles $n(z)$ and $n(x, y)$ remain practically unchanged during and after the uniform motion during 5 ms; this demonstrates the dynamical stability and the mobility of the solitons.

IV. SUMMARY

We demonstrated, using an improved mean-field model including a higher-order LHY repulsive interaction [51] as modified for dipolar systems [52,53] in the GP model equation, that in a very strongly dipolar BEC of NaCs molecules [13], one can have a metastable (excited state) two- and a four-droplet quasi-1D soliton axially free to move along the z direction. These solitons are subject to an expulsive Gaussian potential and a weak harmonic potential, both in the x-y plane. In this study, the dipolar and scattering lengths were taken to be $a_{dd} = 2000a_0$ and $a = 100a_0$, and the number of molecules was kept between 1000 and 4000. The ground state of this system is a one-droplet soliton. The two-droplet (four-droplet) soliton is the first (second) excited state, as illustrated in Fig. 1. The droplets are localized in the x-y plane and elongated along the z-axis, like the droplets in a fully trapped dipolar BEC [15,16], as shown in Fig. 2. The repulsion among (between) the droplets of the four-droplet (two-droplet) soliton, arising due to the combined action of the expulsive Gaussian potential and the dipolar interaction, stabilizes the formation of the soliton. The GP model has a net cubic attractive nonlinear term, and the higher-order LHY interaction leads to a repulsive quartic nonlinearity, which stops the collapse of the strongly dipolar NaCs condensate. These dynamically stable solitons are phase coherent and hence can move as a unified whole along the polarization z direction with a constant velocity, without any relative motion between the droplets, as shown by real-time simulation in Fig. 5, employing the converged imaginary-time wave function as the initial state. To start the motion of the soliton in real-time propagation with a velocity v along z direction, a phase factor of $\exp(izv)$ is printed on the initial state. In this fashion, a two-droplet soliton of $N = 1000$ NaCs molecules and four-droplet soliton of $N = 3000$ NaCs molecules moved 23.5 μm in 5 ms with a linear velocity of 4.7 mm/s, viz. Fig. 5, without any visible deformation of shape, demonstrating the mobility and dynamical stability of the solitons. The four- and two-droplet solitons have a topology distinct from that of a usual one-droplet soliton, and the very large dipole moment of the NaCs molecules has been fundamental in generating these solitons. If the net dipolar interaction of the system is reduced, keeping all other parameters unchanged, the droplets of the present solitons join together to form a one-droplet soliton.

ACKNOWLEDGMENT

S.K.A. acknowledges support by the CNPq (Brazil) Grant Nos. 301324/2019-0 and 303885/2024-6.

DATA AVAILABILITY

The data are not publicly available upon publication because it is not technically feasible and/or the cost of preparing, depositing, and hosting the data would be prohibitive within the terms of this research project. The data are available from the authors upon reasonable request.

[1] T. Lahaye, C. Menotti, L. Santos, M. Lewenstein, and T. Pfau, Rep. Prog. Phys. **72**, 126401 (2009).

[2] T. Lahaye, T. Koch, B. Fröhlich, M. Fattori, J. Metz, A. Griesmaier, S. Giovanazzi, and T. Pfau, Nature (London) **448**, 672 (2007).

[3] A. Griesmaier, J. Stuhler, T. Koch, M. Fattori, T. Pfau, and S. Giovanazzi, Phys. Rev. Lett. **97**, 250402 (2006).

[4] J. Stuhler, A. Griesmaier, T. Koch, M. Fattori, T. Pfau, S. Giovanazzi, P. Pedri, and L. Santos, Phys. Rev. Lett. **95**, 150406 (2005).

[5] K. Goral, K. Rzazewski, and T. Pfau, Phys. Rev. A **61**, 051601(R) (2000).

[6] T. Koch, T. Lahaye, J. Metz, B. Fröhlich, A. Griesmaier, and T. Pfau, Nat. Phys. **4**, 218 (2008).

[7] L. Chomaz, S. Baier, D. Petter, M. J. Mark, F. Wächtler, L. Santos, and F. Ferlaino, Phys. Rev. X **6**, 041039 (2016).

[8] K. Aikawa, A. Frisch, M. Mark, S. Baier, A. Rietzler, R. Grimm, and F. Ferlaino, Phys. Rev. Lett. **108**, 210401 (2012).

[9] M. Lu, S. H. Youn, and B. L. Lev, Phys. Rev. Lett. **104**, 063001 (2010).

[10] J. J. McClelland and J. L. Hanssen, Phys. Rev. Lett. **96**, 143005 (2006).

[11] S. H. Youn, M. W. Lu, U. Ray, and B. L. Lev, Phys. Rev. A **82**, 043425 (2010).

[12] M. Lu, N. Q. Burdick, S. H. Youn, and B. L. Lev, Phys. Rev. Lett. **107**, 190401 (2011).

[13] N. Bigagli, W. Yuan, S. Zhang, B. Bulatovic, T. Karman, I. Stevenson, and S. Will, Nature (London) **631**, 289 (2024).

[14] G. Quéméner, J. L. Bohn, and J. F. E. Croft, Phys. Rev. Lett. **131**, 043402 (2023).

[15] M. Schmitt, M. Wenzel, F. Böttcher, I. Ferrier-Barbut, and T. Pfau, Nature (London) **539**, 259 (2016).

[16] H. Kadau, M. Schmitt, M. Wenzel, C. Wink, T. Maier, I. Ferrier-Barbut, and T. Pfau, Nature (London) **530**, 194 (2016).

[17] F. Wächtler and L. Santos, Phys. Rev. A **93**, 061603(R) (2016).

[18] D. Baillie, R. M. Wilson, R. N. Bisset, and P. B. Blakie, Phys. Rev. A **94**, 021602(R) (2016).

[19] L. Chomaz, D. Petter, P. Ilzhöfer, G. Natale, A. Trautmann, C. Politi, G. Durastante, R. M. W. van Bijnen, A. Patscheider, M. Sohmen, M. J. Mark, and F. Ferlaino, Phys. Rev. X **9**, 021012 (2019).

[20] G. Natale, R. M. W. van Bijnen, A. Patscheider, D. Petter, M. J. Mark, L. Chomaz, and F. Ferlaino, Phys. Rev. Lett. **123**, 050402 (2019).

[21] L. Tanzi, E. Lucioni, F. Famà, J. Catani, A. Fioretti, C. Gabbanini, R. N. Bisset, L. Santos, and G. Modugno, Phys. Rev. Lett. **122**, 130405 (2019).

[22] F. Böttcher, J.-N. Schmidt, M. Wenzel, J. Hertkorn, M. Guo, T. Langen, and T. Pfau, Phys. Rev. X **9**, 011051 (2019).

[23] F. K. Abdullaev, A. Gammal, A. M. Kamchatnov, and L. Tomio, Int. J. Mod. Phys. B **19**, 3415 (2005).

[24] Y. S. Kivshar and B. A. Malomed, Rev. Mod. Phys. **61**, 763 (1989).

[25] O. Bang, W. Krolikowski, J. Wyller, and J. J. Rasmussen, Phys. Rev. E **66**, 046619 (2002).

[26] V. M. Pérez-García, H. Michinel, and H. Herrero, Phys. Rev. A **57**, 3837 (1998).

[27] K. E. Strecker, G. B. Partridge, A. G. Truscott, and R. G. Hulet, Nature (London) **417**, 150 (2002).

[28] L. Khaykovich, F. Schreck, G. Ferrari, T. Bourdel, J. Cubizolles, L. D. Carr, Y. Castin, and C. Salomon, Science **296**, 1290 (2002).

[29] S. L. Cornish, S. T. Thompson, and C. E. Wieman, Phys. Rev. Lett. **96**, 170401 (2006).

[30] M. B. Pandey, P. J. Ackerman, A. Burkart, T. Porenta, S. Žumer, and I. I. Smalyukh, Phys. Rev. E **91**, 012501 (2015).

[31] M. Johansson, A. A. Sukhorukov, and Y. S. Kivshar, Phys. Rev. E **80**, 046604 (2009).

[32] J. Gómez-Gardeñes, B. A. Malomed, L. M. Floría, and A. R. Bishop, Phys. Rev. E **74**, 036607 (2006).

[33] Z. Fan, Y. Shi, Y. Liu, W. Pang, Y. Li, and B. A. Malomed, Phys. Rev. E **95**, 032226 (2017).

[34] H. Sakaguchi, B. Li, and B. A. Malomed, Phys. Rev. E **89**, 032920 (2014).

[35] H. Sakaguchi and B. A. Malomed, Phys. Rev. E **90**, 062922 (2014).

[36] S. Gautam and S. K. Adhikari, Laser Phys. Lett. **12**, 045501 (2015).

[37] L. E. Young-S, P. Muruganandam, and S. K. Adhikari, J. Phys. B **44**, 101001 (2011).

[38] L. D. Carr, J. N. Kutz, and W. P. Reinhardt, Phys. Rev. E **63**, 066604 (2001).

[39] O. L. Berman, R. Y. Kezerashvili, G. V. Kolmakov, and L. M. Pomirchi, Phys. Rev. E **91**, 062901 (2015).

[40] L.-C. Zhao, Phys. Rev. E **97**, 062201 (2018).

[41] N.-S. Wan, Y.-E. Li, and J.-K. Xue, Phys. Rev. E **99**, 062220 (2019).

[42] P. Fang and J. Lin, Phys. Rev. E **109**, 064219 (2024).

[43] M. Salerno and B. B. Baizakov, Phys. Rev. E **98**, 062220 (2018).

[44] Y.-H. Qin, L.-C. Zhao, and L. Ling, Phys. Rev. E **100**, 022212 (2019).

[45] S. K. Adhikari, Phys. Rev. E **104**, 024207 (2021).

[46] M. Guo, F. Böttcher, J. Hertkorn, J.-N. Schmidt, M. Wenzel, H. P. Büchler, T. Langen, and T. Pfau, Nature (London) **574**, 386 (2019).

[47] R. M. Wilson, S. Ronen, and J. L. Bohn, Phys. Rev. A **80**, 023614 (2009).

[48] T. Lahaye, J. Metz, B. Frohlich, T. Koch, M. Meister, A. Griesmaier, T. Pfau, H. Saito, Y. Kawaguchi, and M. Ueda, Phys. Rev. Lett. **101**, 080401 (2008).

[49] N. G. Parker, C. Ticknor, A. M. Martin, and D. H. J. O'Dell, Phys. Rev. A **79**, 013617 (2009).

[50] J. L. Bohn, R. M. Wilson, and S. Ronen, Laser Phys. **19**, 547 (2009).

[51] T. D. Lee, K. Huang, and C. N. Yang, Phys. Rev. **106**, 1135 (1957).

[52] A. R. P. Lima and A. Pelster, Phys. Rev. A **84**, 041604(R) (2011).

[53] R. Schützhold, M. Uhlmann, Y. Xu, and U. R. Fischer, Int. J. Mod. Phys. B **20**, 3555 (2006).

[54] Z. Shi and G. Huang, Phys. Rev. E **107**, 024214 (2023).

[55] F. Wächtler and L. Santos, Phys. Rev. A **94**, 043618 (2016).

[56] R. N. Bisset, R. M. Wilson, D. Baillie, and P. B. Blakie, Phys. Rev. A **94**, 033619 (2016).

[57] R. Kishor Kumar, L. E. Young-S, D. Vudragović, A. Balaž, P. Muruganandam, and S. K. Adhikari, Comput. Phys. Commun. **195**, 117 (2015).
[58] V. I. Yukalov, Laser Phys. **28**, 053001 (2018).
[59] E. Poli, T. Bland, C. Politi, L. Klaus, M. A. Norcia, F. Ferlaino, R. N. Bisset, and L. Santos, Phys. Rev. A **104**, 063307 (2021).
[60] P. B. Blakie, C. Ticknor, A. S. Bradley, A. M. Martin, M. J. Davis, and Y. Kawaguchi, Phys. Rev. E **80**, 016703 (2009).
[61] V. Lončar, L. E. Young-S, S. Škrbić, P. Muruganandam, S. K. Adhikari, and A. Balaž, Comput. Phys. Commun. **209**, 190 (2016).
[62] L. E. Young-S, P. Muruganandam, A. Balaž, and S. K. Adhikari, Comput. Phys. Commun. **286**, 108669 (2023).
[63] P. Muruganandam and S. K. Adhikari, Comput. Phys. Commun. **180**, 1888 (2009).
[64] S. K. Adhikari, Am. J. Phys. **54**, 362 (1986).